Bioactive Materials 37 (2024) 517–532

Contents lists available at ScienceDirect

Bioactive Materials

journal homepage: www.keaipublishing.com/en/journals/bioactive-materials

An orally administered bacterial membrane protein nanodrug ameliorates doxorubicin cardiotoxicity through alleviating impaired intestinal barrier

Zhen Li [a,b,c,1], Junyue Xing [a,b,c,1], Xiaohan Ma [a,b,c,1], Wanjun Zhang [d,1], Chuan Wang [a,b,c], Yingying Wang [a,b,c], Xinkun Qi [c], Yanhui Liu [d], Dongdong Jian [a,b,c], Xiaolei Cheng [f], Yanjie Zhu [g], Chao Shi [h], Yongjun Guo [h], Huan Zhao [e,**], Wei Jiang [a,b,c,*], Hao Tang [a,b,c,***]

[a] National Health Commission Key Laboratory of Cardiovascular Regenerative Medicine, Central China Subcenter of National Center for Cardiovascular Diseases, Henan Cardiovascular Disease Center, Fuwai Central-China Cardiovascular Hospital, Central China Fuwai Hospital of Zhengzhou University, Zhengzhou, 450046, China
[b] Henan Key Laboratory of Chronic Disease Management, Central China Fuwai Hospital of Zhengzhou University, Zhengzhou, Henan, 451464, China
[c] Zhengzhou Key Laboratory of Cardiovascular Aging, Central China Fuwai Hospital of Zhengzhou University, Zhengzhou, Henan, 451464, China
[d] Department of Hematology, Henan Provincial People's Hospital, Zhengzhou, Henan, 450003, China
[e] Department of Oncology, The First Affiliated Hospital of Zhengzhou University, Zhengzhou, China
[f] Department of Anesthesiology, Affiliated Drum Tower Hospital of Medical School of Nanjing University, Nanjing, Jiangsu, 210008, China
[g] Department of Pathology, Central Hospital of Kaifeng City, Kaifeng, Henan, 475000, China
[h] Henan Key Laboratory of Molecular Pathology, Department of Molecular Pathology, The Affiliated Cancer Hospital of Zhengzhou University, Zhengzhou, Henan, 450008, China

ARTICLE INFO

Keywords:
Doxorubicin cardiotoxicity
Intestinal barrier
Protein delivery
Oral nanodrugs
Homeostasis of lymphocytes

ABSTRACT

The cardiotoxicity caused by Dox chemotherapy represents a significant limitation to its clinical application and is a major cause of late death in patients undergoing chemotherapy. Currently, there are no effective treatments available. Our analysis of 295 clinical samples from 132 chemotherapy patients and 163 individuals undergoing physical examination revealed a strong positive correlation between intestinal barrier injury and the development of cardiotoxicity in chemotherapy patients. We developed a novel orally available and intestinal targeting protein nanodrug by assembling membrane protein Amuc_1100 (obtained from intestinal bacteria *Akkermansia muciniphila*), fluorinated polyetherimide, and hyaluronic acid. The protein nanodrug demonstrated favorable stability against hydrolysis compared with free Amuc_1100. The in vivo results demonstrated that the protein nanodrug can alleviate Dox-induced cardiac toxicity by improving gut microbiota, increasing the proportion of short-chain fatty acid-producing bacteria from the *Lachnospiraceae* family, and further enhancing the levels of butyrate and pentanoic acids, ultimately regulating the homeostasis repair of lymphocytes in the spleen and heart. Therefore, we believe that the integrity of the intestinal barrier plays an important role in the development of chemotherapy-induced cardiotoxicity. Protective interventions targeting the intestinal barrier may hold promise as a general clinical treatment regimen for reducing Dox-induced cardiotoxicity.

Peer review under responsibility of KeAi Communications Co., Ltd.

* Corresponding author. National Health Commission Key Laboratory of Cardiovascular Regenerative Medicine, Central China Subcenter of National Center for Cardiovascular Diseases, Henan Cardiovascular Disease Center, Fuwai Central-China Cardiovascular Hospital, Central China Fuwai Hospital of Zhengzhou University, Zhengzhou, 450046, China.

** Corresponding author. Department of Oncology, The First Affiliated Hospital of Zhengzhou University, Zhengzhou, China.

*** Corresponding author. National Health Commission Key Laboratory of Cardiovascular Regenerative Medicine, Central China Subcenter of National Center for Cardiovascular Diseases, Henan Cardiovascular Disease Center, Fuwai Central-China Cardiovascular Hospital, Central China Fuwai Hospital of Zhengzhou University, Zhengzhou, 450046, China.

E-mail addresses: zhaohuan912@126.com (H. Zhao), weijiang@zzu.edu.cn (W. Jiang), tangpku_zzuhao@zzu.edu.cn (H. Tang).

[1] Dr. Z. Li., Dr. J. Xing., Dr. X. Ma., and Dr. W. Zhang contributed equally to this work.

https://doi.org/10.1016/j.bioactmat.2024.03.027
Received 28 September 2023; Received in revised form 7 March 2024; Accepted 20 March 2024

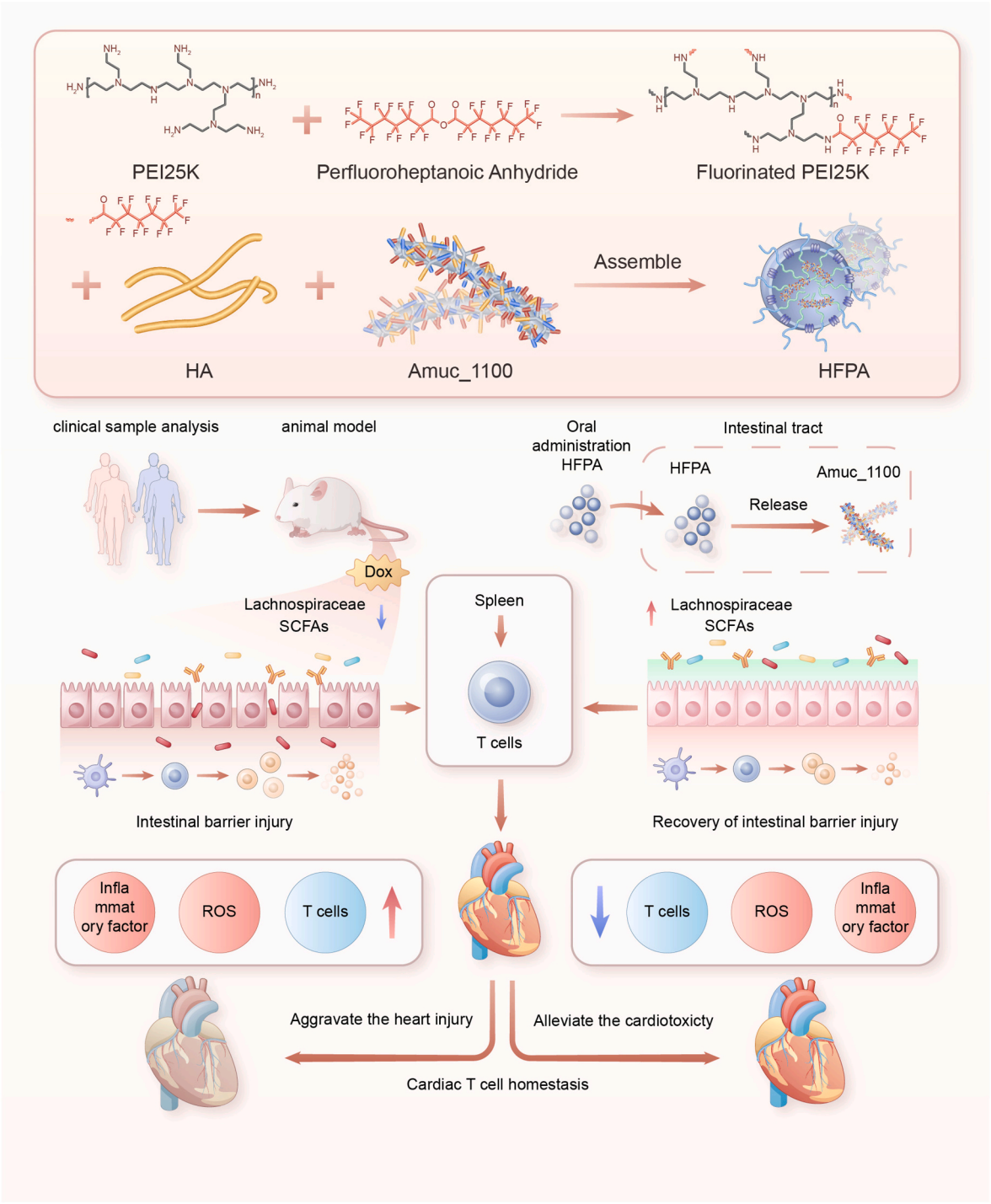

Scheme 1. Diagram depicting the synthesis of the membrane protein drug HFPA and its mechanism in mediating.

1. Introduction

Doxorubicin (Dox) is a powerful anthracycline chemotherapeutic that is commonly used as a first-line treatment for various malignancies, including lymphoma, breast cancer, ovarian cancer, sarcoma and pediatric leukemia. However, the cardiotoxic side effects of Dox, including progressive cardiac dilatation, contractile dysfunction and ultimately heart failure, limit its clinical application [1,2]. Currently, the main strategy for preventing and treating chemotherapy-induced cardiotoxicity is to eliminate or alleviate the direct effect of Dox on cardiomyocytes, through interventions like the preventive use of angiotensin and β-blockers (carvedilol) or the cardioprotective agent dexrazoxane [3]. However, protective interventions based on these related mechanisms have not shown good efficacy in clinical treatment [4]. Treatment with ROS scavengers and iron chelators failed to prevent Dox-induced cardiomyopathy in cancer patients and resulted in significant clinical shortcomings [5]. Specific therapies that can prevent Dox-induced cardiotoxicity are still lacking. Therefore, there is an urgent need for research into rational cardioprotective treatments that effectively reduce the development of Dox-induced cardiotoxicity is urgently needed.

There is growing evidence that the close communication between the

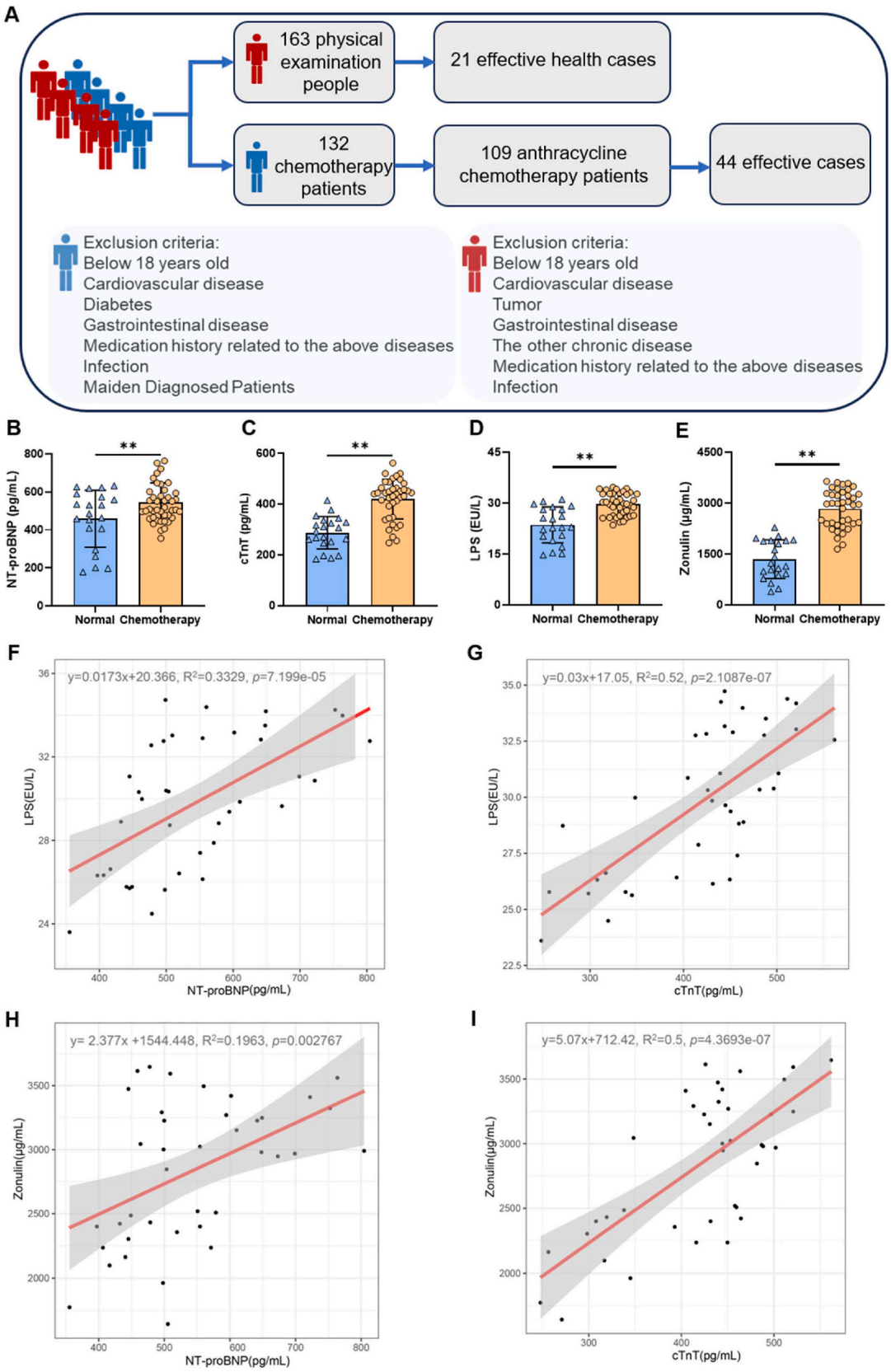

Fig. 1. The analysis of intestinal barrier permeability and cardiotoxicity in chemotherapy patients. (A)The diagram of clinical sample screening process; Plasma NT-proBNP (B), cTnT (C), LPS (D), and zonulin family peptide (E) levels in chemotherapy patients were significantly higher than those in healthy controls. Simple linear regression analysis showed that the levels of LPS (F and H) and zonulin (G and I) were positively correlated with plasma NT-proBNP and cTnT levels. Using *t*-test to analyze the statistical differences. * *P*-value <0.05, ** *P*-value <0.01.

Table 1
Correlation between characteristics of clinical samples and risk factors.

	Health people (n = 21)	Chemotherapy patients (n = 44)			*P*-value
		Pre-Chemocardiotoxicity (n = 23)	Chemocardiotoxicity (n = 16)	High-Chemocardiotoxicity (n = 5)	
Gender (Male/Female)	10/11	11/12	10/6	3/2	0.4149
Age (mean, range)	36.14 ± 10.04	42.43 ± 13.52	57.69 ± 11.35	58.8 ± 18.39	0.0004
Drinking	2/21	3/23	5/16	2/5	0.3631
Smoking	3/21	5/23	5/16	2/5	0.2538
Number of chemotherapies	NA	6.17 ± 3.46	7.38 ± 5.39	8.2 ± 5.07	NA
Echocardiography (Cardiac left ventricular dysfunction)	NA	0/23	16/16	5/5	NA
CKMB (0–24 U/L)	NA	14.63 ± 6.91	16.43 ± 8.05	23.84 ± 13.9	NA
#NT-proBNP (pg/mL)	458.72 ± 150.59	*544.86 ± 119.84	*546.40 ± 92.90	**2808.33 ± 189.73	0.0386
#cTnT (pg/mL)	287.47 ± 63.79	*410.6 ± 90.24	*432.72 ± 56.74	**3471.68 ± 999.37	0.0377
#LPS (EU/L)	23.62 ± 5.31	*29.66 ± 3.53	*30.02 ± 2.77	**188.37 ± 18.53	0.0356
#Zonulin (μg/mL)	1348.99 ± 569.6	*2766.79 ± 598.5	*2940.61 ± 495.05	**18941.77 ± 7298.96	0.0096

NA, Not Applicable. "*" represent significant difference between the health people group and each chemotherapy patient group ("*" *P*-value<0.05, "**" *P*-value <0.01). "#" represents ELISA tests results.

gut microenvironment and the heart (known as the gut-heart axis) is crucial for maintaining normal cardiac function [6,7]. Disruptions in gut microecological homeostasis balance, including disturbances in gut microbiota composition and metabolism, as well as damage to the gut barrier, are risk factors that contribute to the onset and progression of cardiovascular diseases [8,9]. This discovery suggests that the gut microenvironment is an ideal target for the prevention and treatment of heart disease. However, some studies have demonstrated that reducing gut bacteria through antibiotic treatment can protect against the development of myocardial cell injury [10,11], while others suggest that antibiotic treatment can be harmful and lead to inflammation and damage [12]. Additionally, given the significance of gut microbiota to human health, depleting gut bacteria with antibiotics will have severe consequences for patients with tumors, as antibiotics can disrupt the normal balance of bacteria in the gut. Probiotics or dietary intervention are alternative approaches to manipulate the gut microbiota for the prevention and treatment of cardiovascular disease [6,13]. However, the high variability and diversity of the host-gut microecosystem, along with the strain-specific effectiveness of probiotics, result in varying efficacy from individual to individual, hindering the practical benefits of probiotics or dietary interventions [14,15].

As a crucial component of the intestinal microenvironment, the intact intestinal barrier plays a vital role in prevent invasive bacteria or toxic agents from entering the systemic circulation, thus maintaining homeostasis [16,17]. Impaired intestinal barrier has been observed in allergic and autoimmune conditions, systemic autoimmune and metabolic conditions, chronic neuropsychiatric conditions and cardiovascular disease [18,19]. Clinical evidence and animal experiments have indicated that intestinal barrier dysfunction is an early event in the pathogenesis of certain diseases, such as arthritis and neurodegenerative disease [20,21]. Dox-induced mucositis increases intestinal barrier permeability and enhances local and systemic inflammatory responses [22]. This situation presents an opportunity to target the intestinal epithelial barrier to mitigate Doxorubicin-induced cardiotoxicity by preventing barrier integrity disruption or restoring the damaged barrier. Amuc_1100 is a versatile outer membrane protein of the highly promising next-generation probiotic *Akkermansia muciniphila*, which has been shown to replicate some of the beneficial functions of *A. muciniphila*. Recent studies have shown that Amuc_1100 is closely associated with inflammation, metabolic and mental-related diseases [23–26]. It has been reported that Amuc_1100 could reduce obesity and improve metabolic syndrome. Additionally, Amuc_1100 can alleviate ulcerative colitis and colitis associated colorectal cancer through modulation of cytotoxic T lymphocytes [23]. In both clean and obese mice, Amuc_1100 suppressed the inflammation response of macrophages infected by *Porphyromonas gingivali,* leading to reduced periodontal tissue damage and systemic inflammation [27]. Additionally, Amuc_1100 also plays a crucial role in regulating the immune response and maintaining the integrity of the gut barrier through its interaction with TLR2 [28]. However, it is still unclear whether Amuc_1100 could attenuate the leakiness of gut barrier and cardiotoxicity induced by Dox is still unclear. Another primary problem with the translational and commercial development of Amuc_1100 protein drugs is the unsatisfied therapeutic effect caused by enzymatic degradation and rapid clearance *in vivo*. Therefore, there is an urgent need to develop a novel strategy for efficient delivery of Amuc_1100 to intestinal barrier.

This study aims to investigate the correlation between intestinal barrier damage and cardiotoxicity during Dox chemotherapy in both human and mouse models. Additionally, we aim to explore the potential of Amuc_1100 in protecting against Dox-induced cardiotoxicity, based on its known role in safeguarding the intestinal barrier. To overcome the limitations of protein-based drugs, we first synthesized fluorinated polyetherimide (FPEI) and used it to assemble with Amuc_1100 and hyaluronic acid (HA), resulting in the creation of orally available membrane protein nanodrugs (HFPA) with efficient intestinal targeting capability (Scheme 1) [29]. Additionally, we systematically evaluated the HFPA platform's ability to ameliorate impaired intestinal barrier function, and discussed its impact on intestinal microecology and the immunological mechanisms involved in improving cardiac function. Building on these findings, we aim to propose general clinical preventive and protective measures to alleviate Dox-induced cardiotoxicity by focusing on protecting the intestinal barrier.

2. Results and discussion

2.1. Intestinal barrier impairment is associated with the onset of anthracycline-induced cardiotoxicity

Troponin T (cTnT) serves as a key marker for myocardial injury [30,31]. Plasma lipopolysaccharides (LPS) levels have been utilized as an indicator of bacterial translocation, reflecting intestinal barrier permeability [18]. Zonulin, a precursor of the haptoglobin protein that increases intestinal epithelial barrier permeability by downregulating tight junction function [32,33]. Several studies have confirmed that plasma zonulin levels are suitable for assessing intestinal permeability in patients with inflammatory bowel disease (IBD) and autoimmune arthritis [20,32]. Increased intestinal permeability has been observed in cardiovascular diseases (CVDs), such as hypertension, coronary heart disease, and myocardial infarction [18,34]. To investigate the correlation between chemotherapeutic cardiotoxicity and the intestinal barrier, we assessed plasma NT-proBNP, cTnT, LPS and zonulin levels in two independent cohorts of 44 chemotherapy patients and 21 healthy

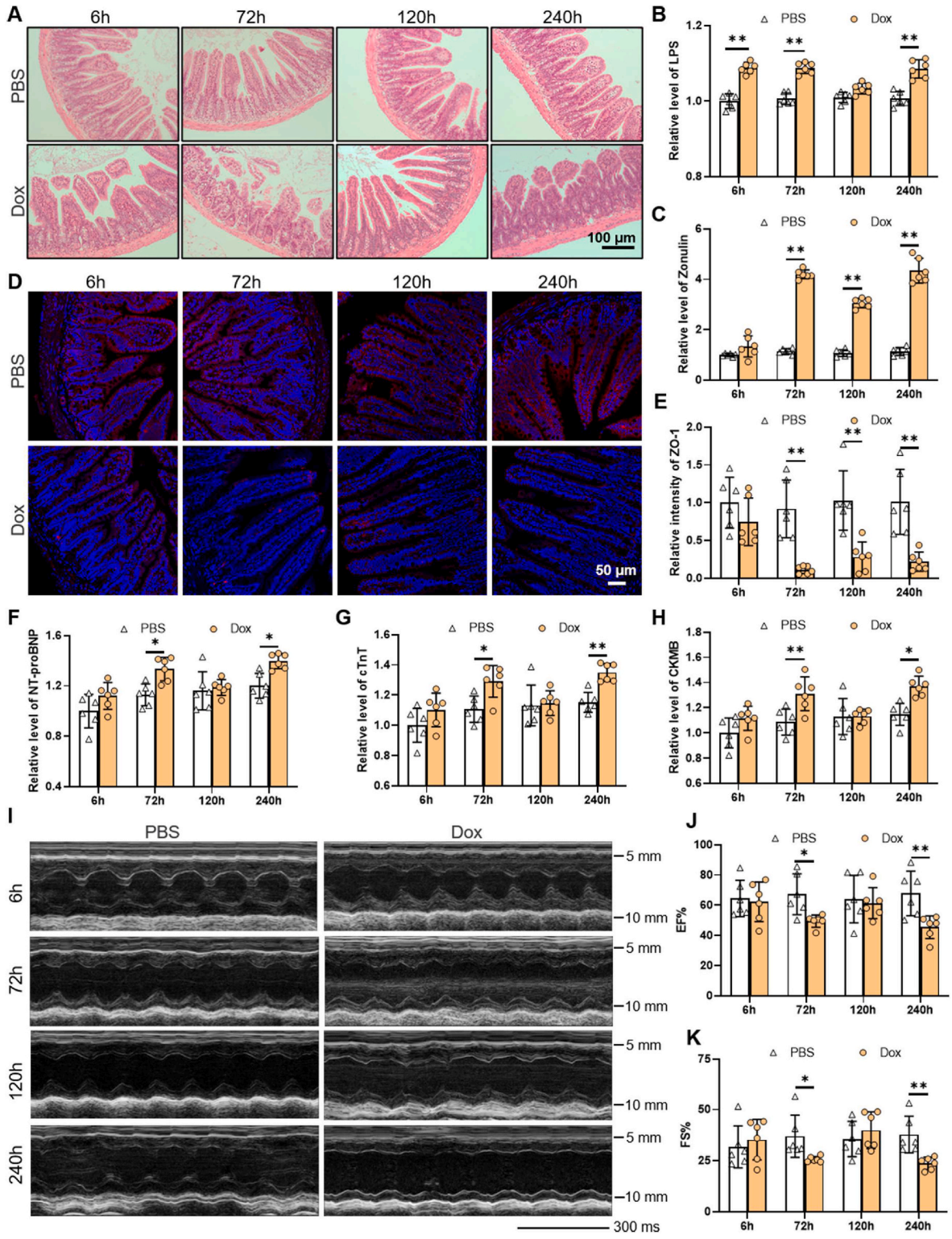

Fig. 2. Dox-induced intestinal barrier injury precedes the onset of abnormal heart function. (A) H&E staining showed the dynamic process of ileal morphology injury induced by Dox during 6–240 h. Scale bar: 100 μm; Dynamic changes in serum LPS (B) and zonulin levels and (C); (D–E) Immunofluorescence images of ileal sections: nuclei, DAPI (blue); ZO-1 (red), Scale bar: 50 μm. (F–H) Plasma levels of the cardiac injury markers NT-proBNP, cTnT, and CKMB; (I–K) Echocardiographic analysis of cardiac function in mice treated by Dox and PBS during 6–240 h, respectively. EF, ejection fraction; FS, fractional shortening. n = 6 mice/group, mean ± SD, and statistical significance was analyzed using the two-way ANOVA followed by Tukey's multiple comparison. * *P*-value <0.05, ** *P*-value <0.01.

control (Fig. 1A). We found that the plasma levels of NT-proBNP, cTnT, LPS, and zonulin in chemotherapy patients were significantly higher than those in healthy controls (Fig. 1B–E and Table 1), and the levels of LPS and zonulin were positively correlated with plasma NT-proBNP and cTnT levels (Fig. 1F–I). Moreover, we identified that patient age may play a crucial role in the onset and progression of cardiotoxicity (Table .1). This could be due to the reduction in myocardial volume as a result of aging-related cardiomyocyte loss, or the substantial increase in

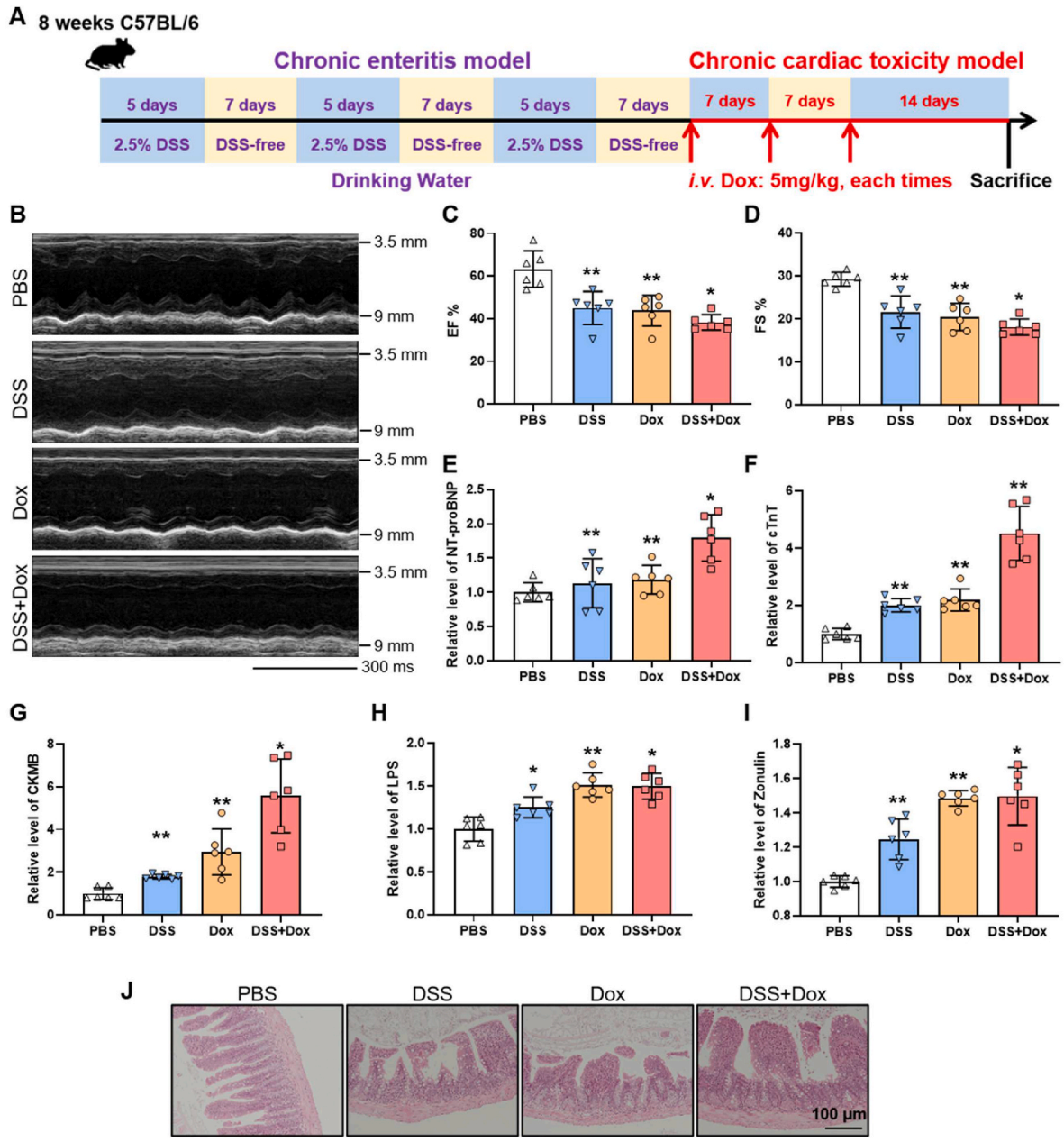

Fig. 3. Early intestinal barrier injury can aggravate Dox cardiotoxicity. (A) Schematic protocol for mice treatments. 2.5% DSS was administered in sterile drinking water every 5 days followed by 7 days of DSS-free water for 3 cycles to induce chronic enteritis model; (B–D) Estimation on cardiac function of mice treated by PBS, Dox, DSS and DSS + Dox echocardiography; (E–G) Plasma levels of the cardiac injury markers NT-proBNP, cTnT, and CKMB; (H–I) Plasma levels of LPS and zonulin; (J) Estimation on ileal histopathology morphology of mice based on H&E staining. Scale bar: 100 μm; EF, ejection fraction; FS, fractional shortening. n = 6 mice/group, mean ± SD, and statistical significance was analyzed using the two-way ANOVA. * *P*-value <0.05, ** *P*-value <0.01.

doxorubicin concentration in the heart caused by the pharmacokinetic changes of anthracycline in elderly chemotherapy patients [35,36]. Furthermore, plasma NT-proBNP, cTnT, LPS, and zonulin levels were significantly elevated in a subset of chemotherapy patients who had not yet developed cardiac dysfunction by echocardiography ("pre--Chemocardiotoxicity"). (Figs. S1A–D). These findings suggest that the intestinal permeability of tumor patients undergoing chemotherapy is compromised, and alterations intestinal permeability appear to precede the occurrence of cardiac dysfunction.

2.2. *Intestinal barrier injury induced by dox precedes the onset of abnormal heart function*

We then conducted a time course analysis of intestinal barrier dysfunction and reduction in cardiac function in mice. Following the first dose, Dox caused noticeable and rapid histopathological changes, including villus blunting within 6 h of injection, followed by significant degeneration of villi and crypts 72 h later, and a subsequent repair phase during which villi lengthened, and crypts regenerated and became hypertrophic (Fig. 2A). Damage to the ileal epithelium was induced again after the second injection after 120 h treated by Dox. The dynamic process of Dox-induced changes in ileal morphology described here was consistent with previous studies [37]. Corresponding to the aforementioned changes in ileal morphology, the intestinal barrier in Dox-treated mice also exhibited dynamic permeability, as indicated by the serum levels of LPS and zonulin (Fig. 2B and C). Furthermore, decreased levels and staining intensity of ZO-1 were observed in Dox-induced small intestinal mucositis (Fig. 2D and E).

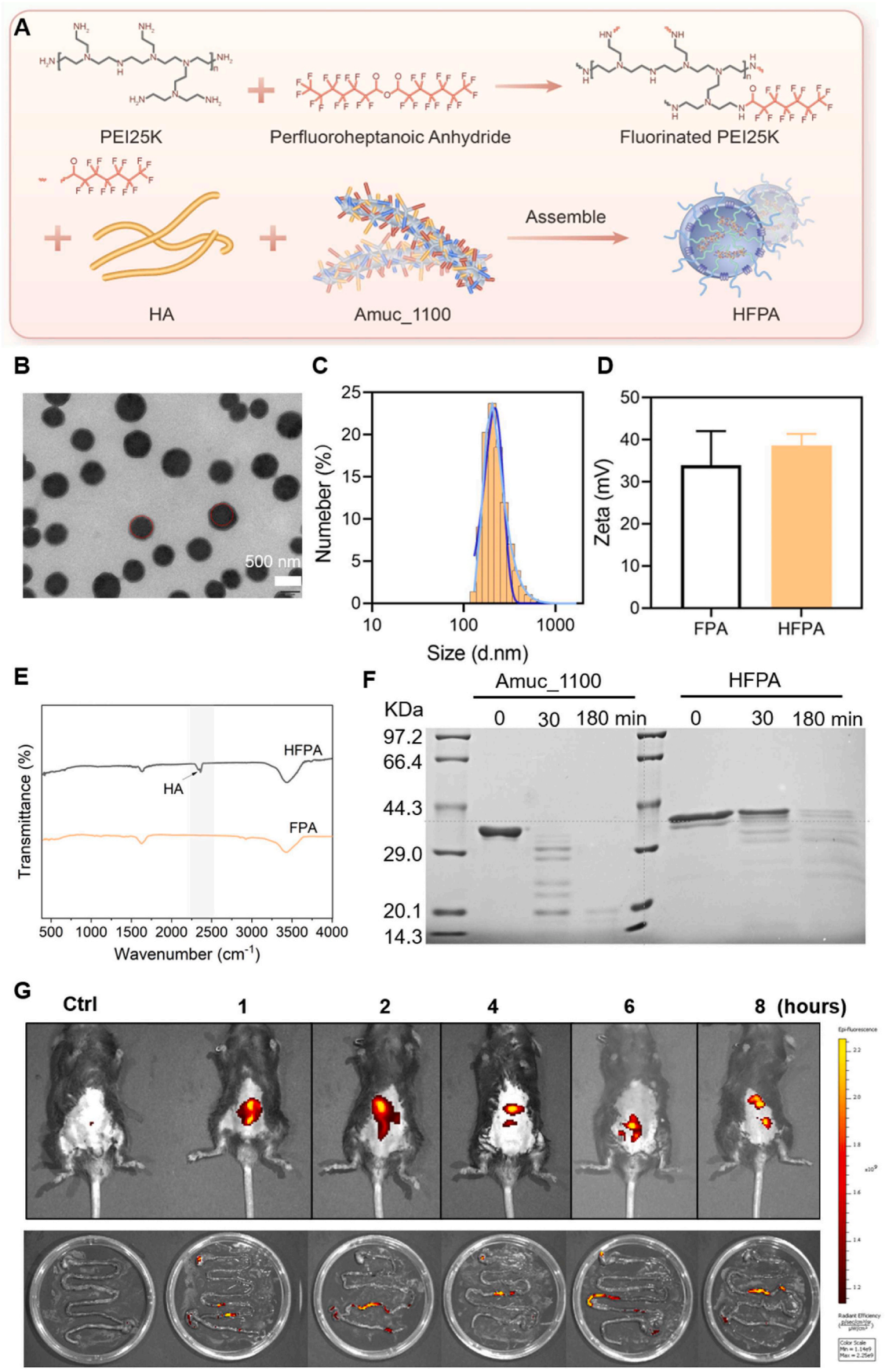

Fig. 4. Characterization of HFPA. (A) Procedure for HFPA synthesis. (B) TEM image of HFPA. (C) Size of HFPA. (D) Zeta potential of HFPA and FPA. (E) FTIR of HFPA and FPA. (F) SDS-PAGE analysis from Amuc_1100 and HFPA treated by trypsin (0–180 min). (G) HFPA in mice and intestinal tract at different time.

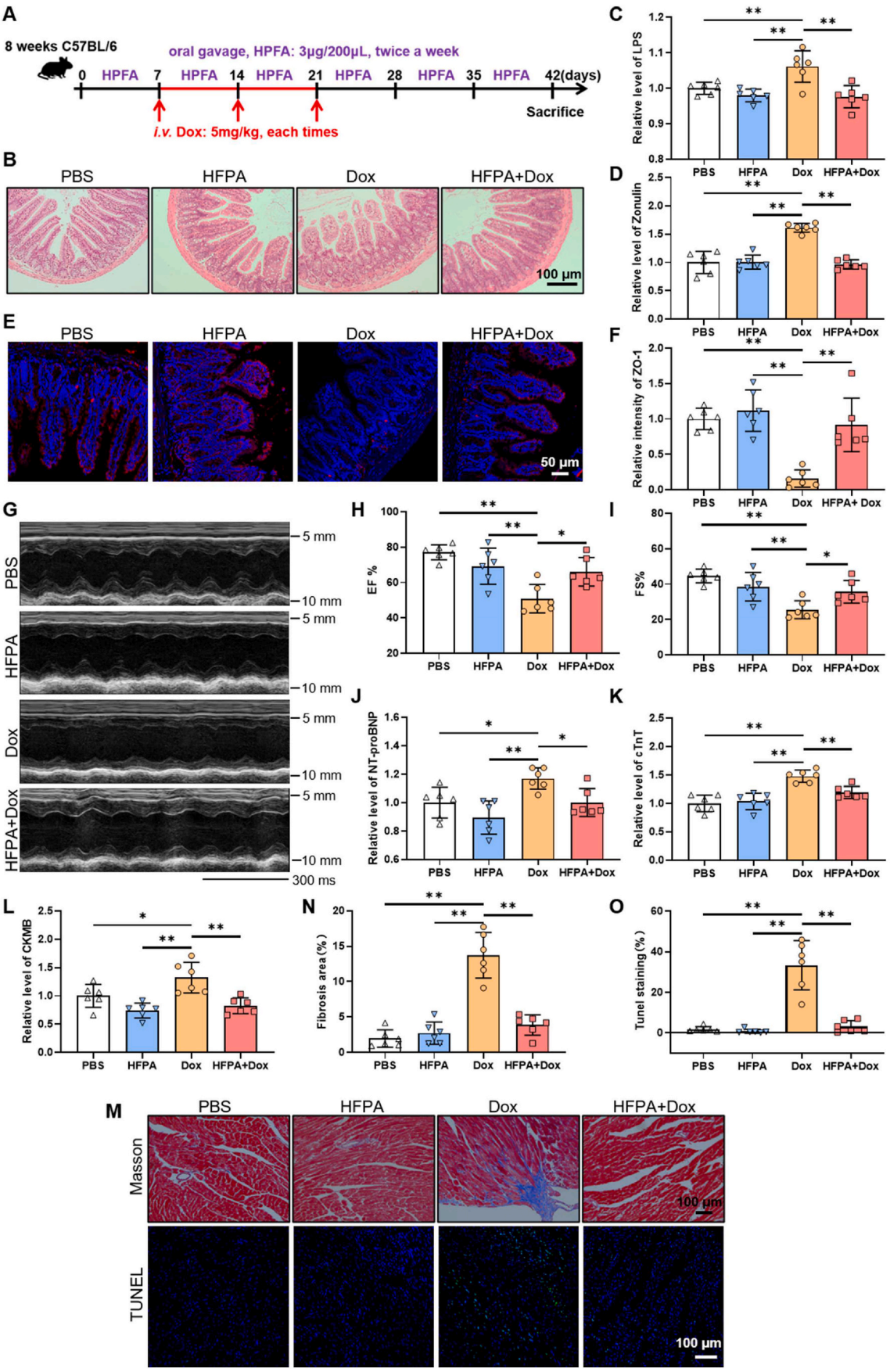

(caption on next page)

Fig. 5. HFPA enhances intestinal barrier integrity and alleviates cardiac dysfunction, myocardial fibrosis and apoptosis in Dox-treated mice. (A) Schematic protocol for mice treatments. Mice were injected intravenously with a cumulative dose of 15 mg/kg Dox three times in 21 days to construct chronic Dox cardiotoxicity model. The mice were respectively treated twice a week with HFPA (3 μg/200 μL) by oral gavage for 7 days before the first Dox treatment; (B) Estimation on ileal histopathology morphology of Dox mice after HFPA intervention based on H&E staining. Scale bar: 100 μm; (C–D) Plasma levels of LPS and zonulin; (E–F) Immunofluorescence images of ileal sections: DAPI (blue); ZO-1 (red). Scale bar: 50 μm; (G–I) Echocardiographic analysis the differences of cardiac function in mice treated by HFPA and the other groups. EF, ejection fraction; FS, fractional shortening; (J–L) Plasma levels of the cardiac injury markers NT-proBNP, cTnT, and CKMB; (M – O) Myocardial fibrosis and cardiomyocyte apoptosis was evaluated by Masson staining and TUNEL staining. n = 6 mice/group, mean ± SD, and statistically analyzed using one-way ANOVA followed by Tukey's multiple comparison. * *P*-value <0.05, ** *P*-value <0.01.

Correspondingly, we evaluated the cardiac function in mice treated with Dox at same time point. Fig. 3 demonstrates a significant increase in plasma cTnT levels and myocardial zymogram (CKMB and NT-proBNP) in Dox-treated mice from 72 h to 240 h post-treatment (Fig. 2F, G and H). However, echocardiography results showed a noticeable decrease in left ventricular ejection fraction (EF%) and fractional shortening (FS%) only at 240 h after Dox injection, with a brief acute injury observed at 72 h (Fig. 2I, J and K). Taken together, the delay between intestinal barrier dysfunction and cardiac dysfunction suggests that Dox-induced disruption of intestinal barrier integrity precedes the onset of cardiac dysfunction. Intestinal injury exhibited a dynamic process of injury, recovery, and reinjury with increasing Dox concentrations and treatment times, similar to previous reports [38]. Dox exposure rapidly induced apoptosis in the intestinal epithelium and mucosal barrier damage in mice, with partial recovery promoted by intestinal crypt stem cells [38]. However, continuous Dox exposure exacerbated cardiotoxicity and led to weakened left ventricular systolic and diastolic function, decreased blood oxygen saturation, increased ischemia and hypoxia, which in turn enhanced intestinal barrier permeability, elevated circulating LPS or inflammatory level, and ultimately exacerbates organ injury [39,40]. Clinical and animal experiments indicate that intestinal barrier damage due to Dox chemotherapy precedes cardiac dysfunction caused by drugs or inflammation, and these factors are interrelated and mutually influence disease occurrence and progression.

2.3. Early intestinal barrier injury can aggravate dox cardiotoxicity

The gut microbiota and intestinal barrier function are disrupted in many clinical tumor patients, indicating an increased risk of Dox-induced cardiotoxicity. To investigate whether intestinal barrier damage exacerbates Dox cardiotoxicity, we induced the DSS-induced mice model of chronic colitis before administering Dox. In brief, mice underwent three cycles of five days of 2.5% DSS administration in sterile drinking water, followed by seven days of DSS-free water (Fig. 3A). Surprisingly, we observed a reduction in cardiac function in mice with chronically increased intestinal barrier permeability. The compromised barrier worsened Dox-induced cardiotoxicity compared to Dox treatment alone (Fig. 3B, C and D). The levels of plasma NT-proBNP, cTnT and CKMB were significantly increased in mice in the DSS, Dox and combination group (Fig. 3E, F and G). Additionally, plasma LPS and zonulin levels were significantly increased in mice in the DSS and Dox combination group (Fig. 3H and I). The H&E staining results demonstrated thickening of intestinal villi and inflammatory cell infiltration in mice in the DSS and Dox combination group (Fig. 3J). These results suggested the importance of assessing the integrity of the intestinal barrier prior to Dox chemotherapy.

2.4. HFPA synthesis and characterization

Based on our findings indicating that a defective intestinal barrier precedes the onset of cardiac dysfunction, our goal was to develop an intervention that could improve intestinal barrier function and potentially alleviate or prevent the onset of cardiac dysfunction. Amuc_1100, a membrane protein derived from *Akkermansia muciniphila* MucT (ATTC BAA-835), which has been demonstrated to regulate tight junction proteins to maintain intestinal barrier homeostasis, was selected as a candidate for potential intervention. In order to achieve efficient delivery of the membrane protein Amuc_1100, fluorinated polyetherimide (FPEI) was synthesized based on previous work and confirmed by nuclear magnetic resonance (^{1}H NMR, Fig. S2). The results of ^{1}H NMR indicate that all amino groups of polyetherimide were successfully fluorinated. The membrane protein drug (HFPA) was fabricated through electrostatic self-assembly using FPEI, Amuc_1100, and hyaluronic acid (HA) as modules (Fig. 4A). The size and morphology of HFPA were examined with a transmission electron microscope (TEM). HFPA particles were spherical, 200–300 nm in diameter, and had a uniform size distribution (Fig. 4B). HFPA exhibited monodispersed spherical morphology with diameters of approximately 200 nm, and the double-layer structure can also be clearly observed under TEM. Dynamic light scattering was used to determine the hydrate particle size (DLS) of HFPA, which were ~208.5–229.8 nm (Fig. 4C). After being assembled with HA, the zeta potential of Ru MOF nanozymes increased from ~ −33.93–~38.64 mV. Protein gel electrophoresis analyses of the HFPA and free Amuc_1100 treated by trypsin (Fig. 4F), which suggests that the membrane protein drug showed enhanced hydrolysis stability, further confirming the successful assemble of Amuc_1100 in the nanoparticle. Additionally, we used an animal fluorescence imaging system to evaluate the *in vivo* retention and distribution of Cy5.5-labeled HFPA in mice. As shown in Fig. 4G, HFPA-Cy5.5 exhibited fluorescence in the intestine for up to 8 h, indicating enhanced retention and intestinal targeting of HFPA.

2.5. HFPA prevents dox-induced intestinal barrier injury and alleviate cardiotoxicity

In our study, we orally supplemented HFPA to improve cardiac function in a Dox-induced chronic cardiotoxicity model (Fig. 5A). We observed that HFPA significantly alleviated Dox-induced histological damage in the ileum, including villi shortening, crypt depth and inflammatory cell infiltration (Fig. 5B). Moreover, HFPA reduced LPS and zonulin levels in serum (Fig. 5C and D). Treatment with HFPA mitigated the decline in the expression levels of tight junction proteins ZO-1 in the ileum of Dox-treated mice (Fig. 5E and F). Echocardiography results demonstrated that HFPA significantly attenuated the Dox-induced decrease in left ventricular (LV) EF% and FS% values (Fig. 5G, H and I). Similarly, the increased plasma levels of NT-proBNP, cTnT, and CKMB caused by Dox were also significantly decreased by HFPA (Fig. 5J, K and L). Masson staining revealed that HFPA decreased the area of cardiac fibrosis in Dox-treated mice (Figure.5M, N), while TUNEL staining showed that HFPA suppressed Dox-induced myocardial apoptosis (Figure.5M, O). However, we observed that HFPA did not ameliorate body weight loss and changes in the heart-body weight ratio (HW/BW) and heart-tibial ratio (HW/TL) (Figs. S3A, B, and C). Nevertheless, the spleen-body weight index SW/BW in Dox-treated mice decreased significantly (Fig. S3D). These results indicate that HFPA treatment could ameliorate Dox-induced ileal mucositis, reduce the permeability of the intestinal barrier, and alleviate cardiotoxicity.

2.6. Oral HFPA administration attenuated dox-induced gut microbial dysbiosis and inflammation

Intestinal microorganisms reside in the intestinal microenvironment and interact with the intestinal mucosal barrier in complex ways.

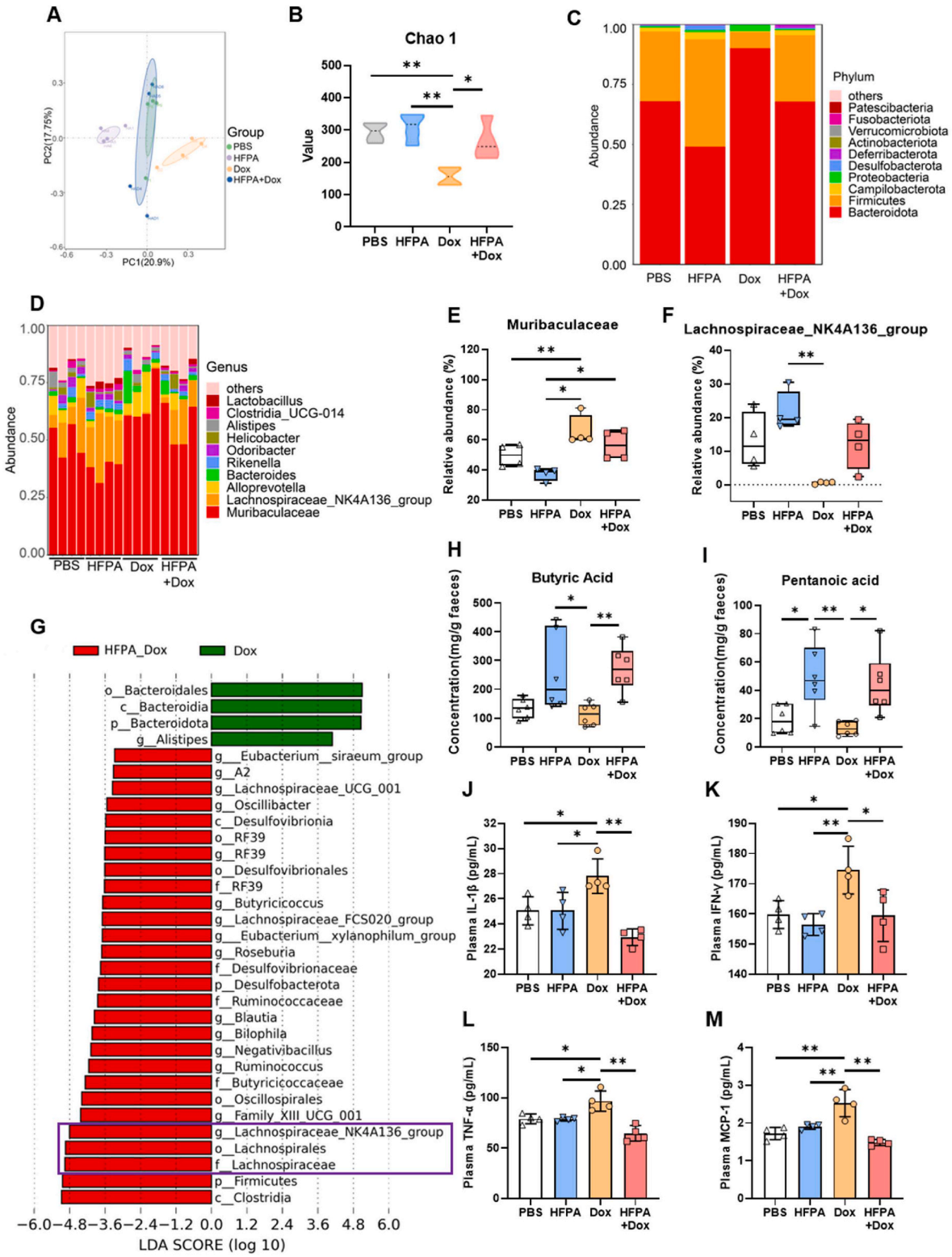

Fig. 6. Oral HFPA administration attenuated Dox-induced gut microbial dysbiosis and inflammation. (A) PCoA was conducted to visualize differences in the fecal microbiota structure among the four groups; (B) α-diversity (Chao1 index) of the intestinal microbiota; (C–D) Relative abundance of intestinal microbiota constituents at the phylum and genus levels; (E–F) Species with significant differences in relative abundance at the genus level; (G) Analysis of the differences in the intestinal microbiota by LEfSe (LDA score≥3 , *P*-value <0.05); (H–I) Contents of butyric acid and pentanoic acid in feces of mice; (J–M) Inflammatory cytokines IL-1β, IFN-γ, TNF-α and MCP-1 levels in plasma, respectively. Values are expressed as mean ± SD; n = 4–6 mice/group. Statistical significance was analyzed using the one-way ANOVA followed by Tukey's multiple comparison. * *P*-value <0.05, ** *P*-value <0.01.

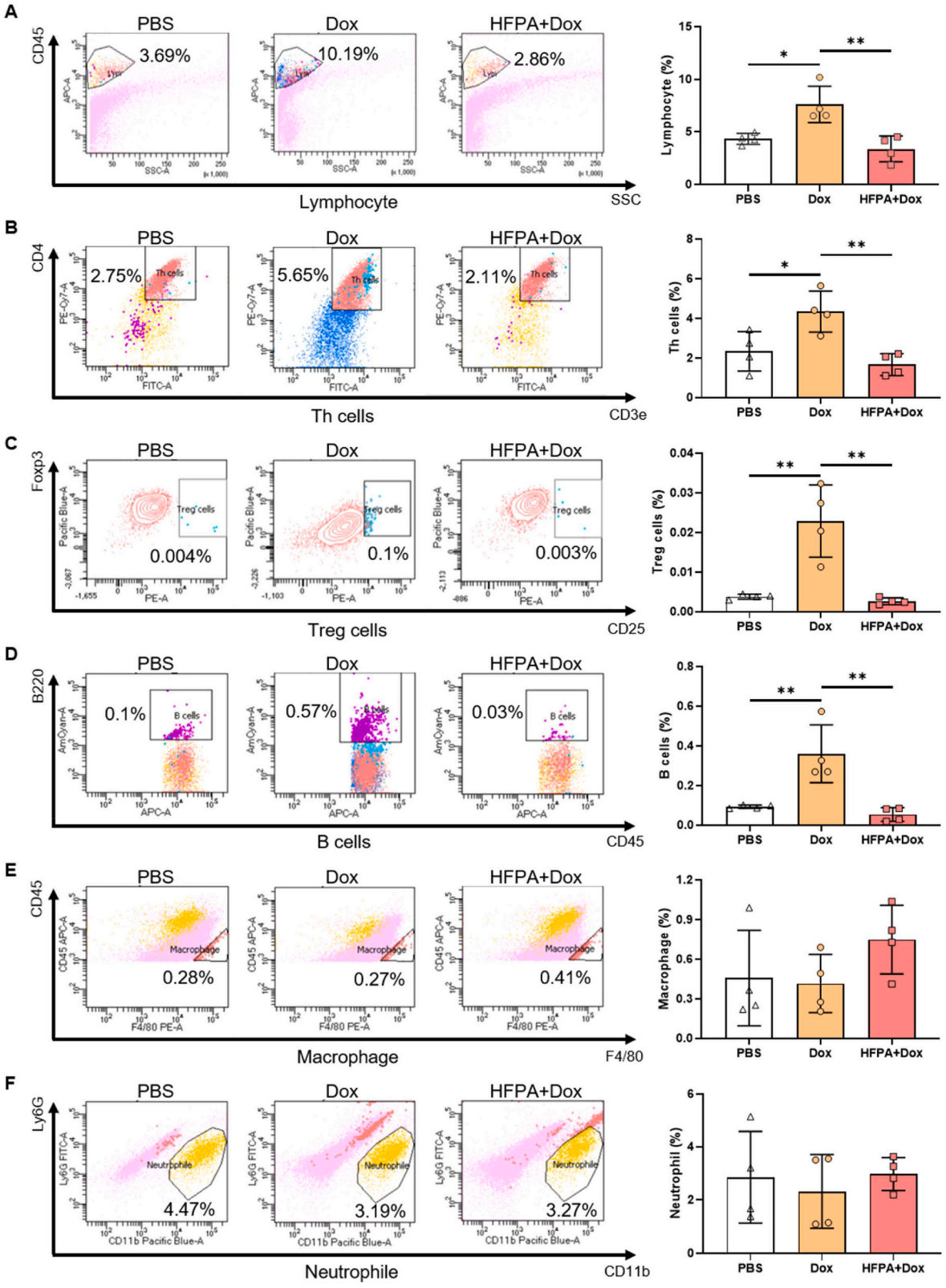

Fig. 7. HFPA alleviates Dox cardiotoxicity by remodeling the composition of cardiac immune cells. (A–D) Proportion of lymphocyte (Lymphocyte, B, Th, Treg cells) and (E–F) myeloid derived immune cells (Macrophage and Neutrophil) in the heart. n = 4 mice/group, mean ± SD. Statistically analyzed using one-way ANOVA followed by Tukey's multiple comparison. * *P*-value <0.05, ** *P*-value <0.01.

Research has demonstrated that intestinal microorganisms play a crucial role in the development of intestinal mucositis caused by Dox chemotherapy, potentially through the elevation of in immunomodulatory chemokines and immune cells in the intestine [22]. While certain studies have indicated that Dox treatment does not have a considerable impact on bacterial growth in vitro [38], it can change the composition of specific bacteria in the intestinal environment, leading to a disruption of the gut microecology [41,42]. It remains unclear whether HFPA can restore the disrupted gut microbiome caused by Dox therapy and improve consequential damage to both the gut barrier and cardiac function is still unclear. T In order to investigate this matter, 16 S rRNA gene sequencing was conducted to assess the impact of oral HFPA administration on the composition and abundance of the intestinal microbiota. Principal components analysis (PCoA) was initially performed to visualize variations in the fecal microbiota structure among the four groups. As anticipated, there were significant differences in the fecal microbiota structure between the mice in the Dox group and those in the other three groups. The microbiota structure of the HFPA + Dox and PBS groups were more similar compared to other groups, whereas the microbiota structure of the group receiving oral HFPA supplement remained distinctive (Fig. 6A). The α-diversity (represented by Chao1 index) of the intestinal microbiota in Dox-treated mice significantly declined (Fig. 6B). These results suggested that Dox significantly altered the gut microbiota structure; however, administering HFPA effectively mitigated the drastic shift in gut microbiota.

We then analyzed the differences in community structures of the four groups of mice at phylum and genus levels. At the phylum level, *Firmicutes* and *Bacteroidetes* were the main phyla across all groups. We found that the relative abundance of *Bacteroidetes* was significantly upregulated and the level of *Firmicutes* was significantly downregulated in the Dox-treated group of mice (Fig. 6C and Figs. S4A and B). At the genus level, *Muribaculaceae*, and *Lachnospiraceae*_NK4A136_group are two genera with relatively high abundance (Fig. 6D), with *Muribaculaceae* being the dominant genus across all groups and having the highest proportion in the Dox group of mice (>60%) (Fig. 6E and Fig. S4G). The proportion of *Lachnospiraceae_NK4A136_group* was significantly decreased in the Dox group of mice compared to the other three groups (Fig. 6F and Fig. S4G). Additionally, while there were no statistically significant differences in the relative abundances of other major bacterial phyla, such as *Proteobacteria*, *Campilobacterota*, *Desulfobacterota* and *Deferribacterota* between the Dox group and the others (Figs. S4C–F).

Further analysis using LEfSe identified significantly different species between the Dox group and the HFPA + Dox group (LDA score≥3, *P*-value <0.05). The results showed that *Bacteroidia* class, *Bacteroidota* phylum, *Alistipes* genus, and *Bacteroidales* order were significantly enriched in the Dox group, and all belonged to the *Bacteroidota* phylum. In contrast, the top 5 enriched bacterial species in the HFPA + Dox group mainly belonged to the *Clostridia* class, *Firmicutes* phylum, *Lachnospiraceae* family, *Lachnospirales* order, and *Lachnospiraceae_NK4A136_group* genus. This was the most significant enrichment found in this group (Fig. 6H), and mostly classified under the *Lachnospirales* order and the *Firmicutes* phylum. The evolutionary tree also showed that the significantly changed microbial differential species mainly belonged to the *Bacteroidales* orders, and *Desulfovibrionaceae* familiy, *RF39* family, *Lachnospiraceae* family, and *Ruminococcaceae* family (Fig. S4H). The aforementioned results suggest that HFPA can restore the dysbiosis caused by Dox, and *Lachnospiraceae* may be a key genus in HFPA-mediated mitigation of Dox-induced intestinal and cardiac toxicity.

Multiple studies have demonstrated that *Lachnospiraceae* can regulate the body's immune and inflammatory responses [43–46] through production of substantial amount of SCFAs [47,48]. Our targeted metabolomic analysis revealed significantly higher levels of butyric acid and pentanoic acid in the feces of mice treated with HFPA compared to those in the Dox group. The levels of acetic acid, propionic acid, and hexanoic acid exhibited an increasing trend, although there was no significant change observed (Fig. 6H, I and Figure S5A, B and C). Additionally, there was a significant increase in the content of isobutyric acid and isovaleric acid (Figs. S5D and E). We examined the levels of inflammatory cytokines IL-1β, IFN-γ, TNF-α, and MCP-1 in plasma to determine the changes in the body's inflammatory state following intervention with HFPA. Our findings indicated that the levels of these inflammatory factors in the mice treated with HFPA were significantly lower compared to the Dox group (Fig. 6I-L). Furthermore, the spleen plays a crucial role in the immune system, and both acute and chronic administration of Dox can impact the immune status of the spleen [49,50]. We used ELISA to measure the levels of IFN-γ and IL-4 in spleen suspensions. The results indicated a notable increase in IFN-γ content in the spleens of mice treated with Dox. However, after HFPA intervention, these levels returned to normal (Fig. S5F). There was no significant difference in the level of IL-4 in the spleen among the four groups of mice (Fig. S5G). Flow cytometric analysis of immunocytes was performed on single-cell suspensions from the spleen (Figs. S6A and S7). The results showed that Dox significantly reduced the proportion of lymphocytes, including $CD4^+$ T cells (Th cells) and B cells, in the spleen. Nonetheless, HFPA intervention effectively restored their proportions to normal levels (Figs. S6B and C). Furthermore, Dox treatment led to a tendency for an increase in the proportion of myeloid-derived cells, such as macrophages and neutrophils. Following HFPA intervention, a significant decrease in the proportion of both macrophages and neutrophils was observed (Figs. S6D and E).

Overall, the findings indicate that HFPA has the potential to improve the imbalance of intestinal microbiota induced by Dox, by enhancing the presence of significant *Lachnospiraceae* genera that produce short-chain fatty acids. This action can help reduce the systemic inflammation triggered by Dox and adjust the immune cell makeup in the spleen.

2.7. HFPA alleviates dox cardiotoxicity by remodeling the composition of cardiac immune cells

Previous research has suggested that the spleen plays a critical role in maintaining and repairing heart homeostasis following Dox treatment [50]. HFPA modulates inflammation levels and spleen immune cell composition by reshaping the gut microbiota. It is also involved in regulating cardiac immune cells. Flow cytometry revealed an increased lymphocyte ratio in the hearts of Dox-treated mice, including B cells, Th cells, and Treg cells. HFPA intervention restored lymphocyte levels to normal (Fig. 7A–D). No significant difference was observed in macrophages and neutrophils of myeloid origin (Fig. 7E and F). Quantification of ROS levels in the heart tissue showed a significant increase in Dox-treated mice, which was markedly decreased after HFPA intervention (Fig. S8A). Real-time qPCR analysis of inflammatory factors in myocardial tissue showed that HFPA intervention significantly reduce the increased expression levels of IL-1β, IFN-γ and TNF-α caused by Dox treatment (Figure. S8B, C and D). These results suggest that chronic Dox treatment elevates the composition ratio of T and B lymphocytes in cardiac tissues. However, the oral administration of HFPA can regulate lymphocyte homeostasis and restore the aforementioned lymphocyte ratios to normal levels.

Previous studies have shown significant increase in $CD8^+$ and $CD4^+$ T cells in the failing heart, as well as an increase in the $CD4^+$ subpopulation of Th1, Th2, Th17, and Treg cells. T present in both the heart and spleen of heart failure patients have been found to be capable of inducing cardiac injury and remodeling [51]. Additionally, it has been observed that T cells are initially recruited from immune organs, such as the spleen, and may contribute to the exacerbation of inflammation in the heart during Dox chemotherapy [50,52]. The spleen serves as a reservoir for T lymphocytes, and activated spleen T lymphocytes have the ability to migrate to the central nervous system, where they can positively regulate the function of the sympathetic nervous system in various organs, thereby exacerbating the inflammatory response and tissue and organ damage [53]. These findings may indicate that the repeated administration of Dox could accelerate the migration of

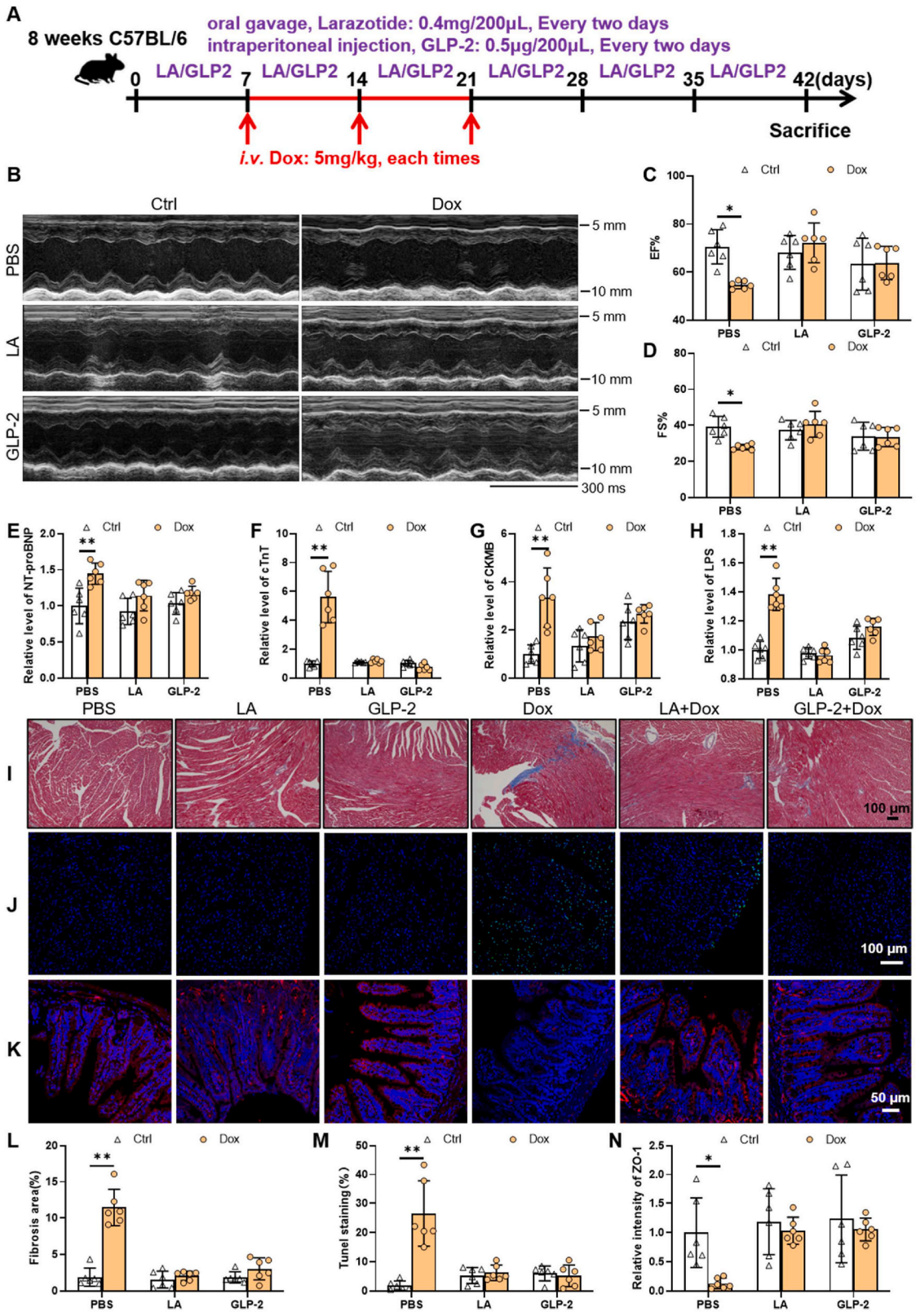

Fig. 8. Protecting the intestinal barrier to alleviate Dox cardiotoxicity may be a general treatment strategy. (A) Schematic protocol for mice treatments. Construction of chronic Dox cardiotoxicity mouse model. The mice were respectively treated every two days with LA (0.4 mg/200 μL) by oral gavage, or GLP-2 (0.5 μg/200 μL) was administrated via intraperitoneal injections; (B–D) Echocardiography showed that LA and GLP-2 also prevented Dox induced left ventricular dysfunction, n = 6 mice/group; (E–G) Plasma NT-proBNP, cTnT, and CKMB levels in Dox mice treated with LA and GLP-2, n = 6 mice/group; (H) LA and GLP-2 significantly decreased plasma LPS levels, n = 6 mice/group; (I, L) Myocardial fibrosis and cardiomyocyte apoptosis were evaluated by Masson staining and (J, M) TUNEL staining; (K, N) Immunofluorescence images of ileal sections: DAPI (blue); ZO-1 (red). Scale bar: 50 μm; n = 6 mice/group. Mean ± SD, and statistically analyzed using two-way ANOVA followed by Tukey's multiple comparison. * *P*-value <0.05, ** *P*-value <0.01.

lymphocytes from the spleen to the injured myocardium. Hence, it is hypothesized that the overactivation or accumulation of lymphocytes in the heart may play a crucial role in Dox-induced cardiotoxicity. HFPA mitigates Dox induced cardiotoxicity by modulating the repair of lymphocyte homeostasis in the spleen and heart.

2.8. Protecting the intestinal barrier to alleviate dox cardiotoxicity may be a general treatment strategy

To further support our hypothesis, we designed LA and GLP-2 as alternative agents to Amuc_1100 for protecting the epithelial barrier and obtained protein nanodrugs. These nanodrugs were systematically evaluated in our study (Fig. 8A) [20,54]. Echocardiography showed that LA and GLP-2 prevented Dox-induced left ventricular dysfunction (Fig. 8B, C and D). Moreover, similar to the intervention effect of HFPA, the plasma NT-proBNP, cTnT, and CKMB, which are indicative of myocardial injury, as well as the LPS levels related to intestinal barrier injury, decreased significantly in Dox-treated mice given LA and GLP-2 (Fig. 8E–H). Immunofluorescence revealed an up-regulation in the expression of ZO-1 in the ileum of mice after intervention (Fig. 8K and N). Histological staining indicated a reduction in myocardial fibrosis (Fig. 8I and L) and cardiomyocyte apoptosis (Fig. 8J and M) in Dox-induced mice were decreased by LA and GLP-2, respectively. These results show that improving intestinal barrier function can effectively alleviate the cardiotoxic side effects caused by Dox. Interventions targeting the intestinal barrier may herald a new approach to cardiotoxic intervention.

3. Conclusion

In conclusion, our study confirmed the significant role of the intestinal barrier in the onset and progression of Dox-induced cardiotoxicity. Targeted protection of intestinal barrier function to alleviate chemotherapy-induced cardiotoxicity is a convenient and effective intervention strategy. Future research should focus on exploring the molecular mechanism of intestinal barrier in the occurrence and protection from Dox chemotherapy-induced cardiotoxicity, and whether this effect is applicable to cardiotoxicity caused by various drugs used for cancer treatment. Additionally, there is a need for extensive screening and identification of probiotics, metabolites, or other functional biological macromolecules associated with intestinal barrier protection, as well as analysis of their protective effects in treating cardiotoxicity caused by Dox chemotherapy. These findings will serve as a foundation for the development and expansion of drugs and intervention methods for Dox chemotherapy-induced cardiotoxicity, ultimately reducing drug side effects and economic burden on chemotherapy patients in clinical practice.

Experimental section

The detailed experimental processes are available in the Supplementary Information.

Ethics approval

The study was approved by the Institutional Ethics Committee of Henan Provincial People's Hospital (Approval number 2020-068-09) and all samples were collected after obtaining informed and written consents from candidates.

All the animal experiments were approved by the Animal Care and Use Committee of Zhengzhou University (No. 2021042501).

Declaration of interest statement

We declare that we have no financial and personal relationships with other people or organizations that can inappropriately influence our work, there is no professional or other personal interest of any nature or kind in any product, service and/or company that could be constructed as influencing the position presented in, or the review of, the manuscript entitled.

Conflict of interest

The authors declare no conflict of interest.

Received: ((will be filled in by the editorial staff)) Revised: ((will be filled in by the editorial staff)) Published online: ((will be filled in by the editorial staff))

CRediT authorship contribution statement

Zhen Li: Writing – review & editing, Writing – original draft, Visualization, Validation, Supervision, Software, Resources, Project administration, Methodology, Investigation, Funding acquisition, Formal analysis, Data curation, Conceptualization. **Junyue Xing:** Writing – review & editing, Writing – original draft, Visualization, Validation, Supervision, Software, Resources, Project administration, Methodology, Investigation, Funding acquisition, Formal analysis, Data curation. **Xiaohan Ma:** Writing – original draft, Visualization, Validation, Supervision, Software, Resources, Project administration, Methodology, Investigation, Formal analysis, Data curation. **Wanjun Zhang:** Writing – review & editing, Visualization, Validation, Supervision, Resources, Project administration, Methodology, Investigation, Formal analysis, Data curation. **Chuan Wang:** Visualization, Supervision, Resources, Methodology, Funding acquisition, Data curation. **Yingying Wang:** Supervision, Software, Project administration, Methodology, Data curation. **Xinkun Qi:** Validation, Software, Project administration, Methodology, Data curation. **Yanhui Liu:** Resources, Methodology, Investigation, Formal analysis. **Dongdong Jian:** Methodology, Investigation, Data curation. **Xiaolei Cheng:** Methodology, Formal analysis, Data curation. **Yanjie Zhu:** Supervision, Project administration, Methodology, Investigation, Funding acquisition. **Chao Shi:** Methodology, Investigation, Data curation. **Yongjun Guo:** Project administration, Methodology. **Huan Zhao:** Writing – original draft, Software, Resources, Funding acquisition, Formal analysis, Data curation, Conceptualization. **Wei Jiang:** Writing – review & editing, Writing – original draft, Validation, Supervision, Resources, Methodology, Investigation, Funding acquisition, Formal analysis, Data curation, Conceptualization. **Hao Tang:** Writing – review & editing, Writing – original draft, Validation, Supervision, Software, Resources, Methodology, Investigation, Funding acquisition, Formal analysis.

Acknowledgments

This work was supported by National Natural Science Foundation of China (No. 32100093, and 82100294), Natural Science Foundation of Henan Province (No.232300421175), Medical Science and Technology Project of Henan Province (SBGJ202302032), Henan Provincial Joint Fund of Science and Technology Research and Development Program (225200810075), and The Young Elite Scientists Sponsorship Program by Henan Association for Science and Technology (Grant 2024HYTP048).

Appendix A. Supplementary data

Supplementary data to this article can be found online at https://doi.org/10.1016/j.bioactmat.2024.03.027.

References

[1] D.N. Jones, J.H. Jordan, G.C. Melendez, Z. Lamar, A. Thomas, D.W. Kitzman, C. Suerken, R.B. D'Agostino Jr., W.G. Hundley, Frequency of transition from stage A to stage B heart failure after initiating potentially cardiotoxic chemotherapy, JACC Heart Fail. 6 (12) (2018) 1023–1032.

[2] C.J. Beavers, J.E. Rodgers, A.J. Bagnola, T.M. Beckie, U. Campia, K.E. Di Palo, T. M. Okwuosa, E.R. Przespolewski, S. Dent, C. American Heart Association Clinical Pharmacology, Cardio-Oncology Committee of the Council on Clinical, C., Council on, G.; precision, M.; the council on peripheral vascular, D., cardio-oncology drug interactions: a scientific statement from the American heart association, Circulation. 145 (15) (2022) e811–e838.

[3] K.T. Sawicki, V. Sala, L. Prever, E. Hirsch, H. Ardehali, A. Ghigo, Preventing and treating anthracycline cardiotoxicity: new insights, Annu. Rev. Pharmacol. Toxicol. 61 (2021) 309–332.

[4] G. Gulati, S.L. Heck, A.H. Ree, P. Hoffmann, J. Schulz-Menger, M.W. Fagerland, B. Gravdehaug, F. von Knobelsdorff-Brenkenhoff, A. Bratland, T.H. Storas, T. A. Hagve, H. Rosjo, K. Steine, J. Geisler, T. Omland, Prevention of cardiac dysfunction during adjuvant breast cancer therapy (PRADA): a 2 x 2 factorial, randomized, placebo-controlled, double-blind clinical trial of candesartan and metoprolol, Eur. Heart J. 37 (21) (2016) 1671–1680.

[5] S.E. Lipshultz, T.R. Cochran, V.I. Franco, T.L. Miller, Treatment-related cardiotoxicity in survivors of childhood cancer, Nat. Rev. Clin. Oncol. 10 (12) (2013) 697–710.

[6] B. Sun, T. Ma, Y. Li, N. Yang, B. Li, X. Zhou, S. Guo, S. Zhang, L.Y. Kwok, Z. Sun, H. Zhang, Bifidobacterium lactis probio-M8 adjuvant treatment confers added benefits to patients with coronary artery disease via target modulation of the gut-heart/-brain axes, mSystems. 7 (2) (2022) e0010022.

[7] S. Ahlawat, Asha, K.K. Sharma, Gut-organ axis: a microbial outreach and networking, Lett. Appl. Microbiol. 72 (6) (2021) 636–668.

[8] Z. Jiang, L.-b. Zhuo, Y. He, Y. Fu, L. Shen, F. Xu, W. Gou, Z. Miao, M. Shuai, Y.J.N. C. Liang, The gut microbiota-bile acid axis links the positive association between chronic insomnia and cardiometabolic diseases, Nat Commun 13 (1) (2022) 3002.

[9] Q. Zhou, J. Deng, X. Pan, D. Meng, Y. Zhu, Y. Bai, C. Shi, Y. Duan, T. Wang, X.J. M. Li, Gut microbiome mediates the protective effects of exercise after myocardial infarction, Microbiome. 10 (1) (2022) 82.

[10] R.J. Rigby, J. Carr, K. Orgel, S.L. King, P.K. Lund, C.M. J.G.m. Dekaney, Intestinal bacteria are necessary for doxorubicin-induced intestinal damage but not for doxorubicin-induced apoptosis, Gut Microbes 7 (5) (2016) 414–423.

[11] L. Wang, Q. Chen, H. Qi, C. Wang, C. Wang, J. Zhang, L.J. C.r. Dong, Doxorubicin-induced systemic inflammation is driven by upregulation of toll-like receptor TLR4 and endotoxin LeakageGut flora promoted doxotubicin-induced, Inflammation. 76 (22) (2016) 6631–6642.

[12] H. Lin, L. Meng, Z. Sun, S. Sun, X. Huang, N. Lin, J. Zhang, W. Lu, Q. Yang, J. Chi, H. Guo, Yellow wine polyphenolic compound protects against doxorubicin-induced cardiotoxicity by modulating the composition and metabolic function of the gut microbiota, Circ Heart Fail. 14 (10) (2021) e008220.

[13] Z. Miao, W. Du, C. Xiao, C. Su, W. Gou, L. Shen, J. Zhang, Y. Fu, Z. Jiang, Z. Wang, X. Jia, J.S. Zheng, H. Wang, Gut microbiota signatures of long-term and short-term plant-based dietary pattern and cardiometabolic health: a prospective cohort study, BMC Med. 20 (1) (2022) 204.

[14] N. Zmora, G. Zilberman-Schapira, J. Suez, U. Mor, M. Dori-Bachash, S. Bashiardes, E. Kotler, M. Zur, D. Regev-Lehavi, R.B.-Z.J.C. Brik, Personalized gut mucosal colonization resistance to empiric probiotics is associated with unique host and microbiome features, Cell 174 (6) (2018) 1388–1405. e21.

[15] T. Du, A. Lei, N. Zhang, C. Zhu, The beneficial role of probiotic lactobacillus in respiratory diseases, Front. Immunol. 13 (2022) 908010.

[16] M. Schwarzfischer, G.J.M. Rogler, The intestinal barrier—shielding the body from nano-and microparticles in our diet, Metabolites 12 (3) (2022) 223.

[17] K.R. Groschwitz, S.P. Hogan, Intestinal barrier function: molecular regulation and disease pathogenesis, J. Allergy Clin. Immunol. 124 (1) (2009) 3–20, quiz 21-2.

[18] C.V. Lewis, W.R. Taylor, Intestinal barrier dysfunction as a therapeutic target for cardiovascular disease, Am. J. Physiol. Heart Circ. Physiol. 319 (6) (2020) H1227–H1233.

[19] Cezmi A Akdis, Does the epithelial barrier hypothesis explain the increase in allergy, autoimmunity and other chronic conditions? Nat Rev Immunol 21 (11) (2021) 739–751.

[20] N. Tajik, M. Frech, O. Schulz, F. Schalter, S. Lucas, V. Azizov, K. Durholz, F. Steffen, Y. Omata, A. Rings, M. Bertog, A. Rizzo, A. Iljazovic, M. Basic, A. Kleyer, S. Culemann, G. Kronke, Y. Luo, K. Uberla, U.S. Gaipl, B. Frey, T. Strowig, K. Sarter, S.C. Bischoff, S. Wirtz, J.D. Canete, F. Ciccia, G. Schett, M.M. Zaiss, Targeting zonulin and intestinal epithelial barrier function to prevent onset of arthritis, Nat. Commun. 11 (1) (2020) 1995.

[21] P. Honarpisheh, C.R. Reynolds, M.P. Blasco Conesa, J.F. Moruno Manchon, N. Putluri, M.B. Bhattacharjee, A. Urayama, L.D. McCullough, B.P. Ganesh, Dysregulated gut homeostasis observed prior to the accumulation of the brain amyloid-β in Tg2576 mice, Int J Mol Sci 21 (5) (2020) 1711.

[22] L. Wang, Q. Chen, H. Qi, C. Wang, C. Wang, J. Zhang, L. Dong, Doxorubicin-induced systemic inflammation is driven by upregulation of toll-like receptor TLR4 and endotoxin leakage, Cancer Res. 76 (22) (2016) 6631–6642.

[23] L. Wang, L. Tang, Y. Feng, S. Zhao, M. Han, C. Zhang, G. Yuan, J. Zhu, S. Cao, Q. Wu, L. Li, Z. Zhang, A purified membrane protein from Akkermansia muciniphila or the pasteurised bacterium blunts colitis associated tumourigenesis by modulation of CD8(+) T cells in mice, Gut. 69 (11) (2020) 1988–1997.

[24] N. Ottman, J. Reunanen, M. Meijerink, T.E. Pietila, V. Kainulainen, J. Klievink, L. Huuskonen, S. Aalvink, M. Skurnik, S. Boeren, R. Satokari, A. Mercenier, A. Palva, H. Smidt, W.M. de Vos, C. Belzer, Pili-like proteins of Akkermansia muciniphila modulate host immune responses and gut barrier function, PLoS One. 12 (3) (2017) e0173004.

[25] H. Plovier, A. Everard, C. Druart, C. Depommier, M. Van Hul, L. Geurts, J. Chilloux, N. Ottman, T. Duparc, L. Lichtenstein, A. Myridakis, N.M. Delzenne, J. Klievink, A. Bhattacharjee, K.C. van der Ark, S. Aalvink, L.O. Martinez, M.E. Dumas, D. Maiter, A. Loumaye, M.P. Hermans, J.P. Thissen, C. Belzer, W.M. de Vos, P. D. Cani, A purified membrane protein from Akkermansia muciniphila or the pasteurized bacterium improves metabolism in obese and diabetic mice, Nat. Med. 23 (1) (2017) 107–113.

[26] Y. Xu, J. Duan, D. Wang, J. Liu, X. Chen, X.-Y. Qin, W.J.M. Yu, Akkermansia muciniphila alleviates persistent inflammation, immunosuppression, and catabolism syndrome in mice. Metabolites 13 (2) (2023) 194.

[27] H. Mulhall, Akkermansia Muciniphila Ameliorates the Host Response to Porphyromonas Gingivalis-Induced Experimental Periodontitis, New York Medical College, 2021.

[28] J. Wang, W. Xu, R. Wang, R. Cheng, Z. Tang, M. Zhang, The outer membrane protein Amuc_1100 of Akkermansia muciniphila promotes intestinal 5-HT biosynthesis and extracellular availability through TLR2 signalling, Food Funct. 12 (8) (2021) 3597–3610.

[29] Y. Lee, K. Sugihara, M.G. Gillilland III, S. Jon, N. Kamada, J.J. J.N.m. Moon, Hyaluronic acid–bilirubin nanomedicine for targeted modulation of dysregulated intestinal barrier, microbiome and immune responses in colitis, Nat. Mater. 19 (1) (2020) 118–126.

[30] D. Lindholm, J. Lindbäck, P. Armstrong, A. Budaj, C. Cannon, C. Granger, E. Hagström, C. Held, W. Koenig, O. Östlund, R. Stewart, J. Soffer, H. White, R. de Winter, P. Steg, A. Siegbahn, M. Kleber, A. Dressel, T. Grammer, W. März, L. Wallentin, Biomarker-based risk model to predict cardiovascular mortality in patients with stable coronary disease, J. Am. Coll. Cardiol. 70 (7) (2017) 813–826.

[31] J. Berry, H. Chen, V. Nambi, W. Ambrosius, S. Ascher, M. Shlipak, J. Ix, R. Gupta, A. Killeen, R. Toto, D. Kitzman, C. Ballantyne, J. de Lemos, Effect of intensive blood pressure control on troponin and natriuretic peptide levels: findings from SPRINT, Circulation. 147 (4) (2023) 310–323.

[32] G.P. Caviglia, F. Dughera, D.G. Ribaldone, C. Rosso, M.L. Abate, R. Pellicano, F. Bresso, A. Smedile, G.M. Saracco, M. Astegiano, Serum zonulin in patients with inflammatory bowel disease: a pilot study, Minerva Med. 110 (2) (2019) 95–100.

[33] T. Vanuytsel, S. Vermeire, I. Cleynen, The role of Haptoglobin and its related protein, Zonulin, in inflammatory bowel disease, Tissue Barriers. 1 (5) (2013) e27321.

[34] S.S. Ghosh, J. Wang, P.J. Yannie, S. Ghosh, Intestinal barrier dysfunction, LPS translocation, and disease development, J. Endocrine Soc. 4 (2) (2020) bvz039.

[35] P. Reddy, C. Shenoy, A.H. Blaes, Cardio-oncology in the older adult, J. Geriatric Oncol. 8 (4) (2017) 308–314.

[36] E.M. Screever, W.C. Meijers, J.J. Moslehi, Age-related considerations in cardio-oncology, J. Cardiovasc. Pharmacol. Therapeut. 26 (2) (2020) 103–113.

[37] A. Kaczmarek, B.M. Brinkman, L. Heyndrickx, P. Vandenabeele, D.V. Krysko, Severity of doxorubicin-induced small intestinal mucositis is regulated by the TLR-2 and TLR-9 pathways, J. Pathol. 226 (4) (2012) 598–608.

[38] R.J. Rigby, J. Carr, K. Orgel, S.L. King, P.K. Lund, C.M. Dekaney, Intestinal bacteria are necessary for doxorubicin-induced intestinal damage but not for doxorubicin-induced apoptosis, Gut Microb. 7 (5) (2016) 414–423.

[39] P.R. de Jong, J.M. González-Navajas, N.J.G. Jansen, The digestive tract as the origin of systemic inflammation, Crit. Care. 20 (1) (2016) 1–12.

[40] M. Huber-Lang, J.D. Lambris, P.A. J.N.i. Ward, Innate immune responses to trauma, Nat. Immunol. 19 (4) (2018) 327–341.

[41] R. Wu, X. Mei, J. Wang, W. Sun, T. Xue, C. Lin, D. Xu, Zn(ii)-Curcumin supplementation alleviates gut dysbiosis and zinc dyshomeostasis during doxorubicin-induced cardiotoxicity in rats, Food Funct. 10 (9) (2019) 5587–5604.

[42] E. Montassier, T. Gastinne, P. Vangay, G.A. Al-Ghalith, S. Bruley des Varannes, S. Massart, P. Moreau, G. Potel, M.F. de La Cochetiere, E. Batard, D. Knights, Chemotherapy-driven dysbiosis in the intestinal microbiome, Aliment. Pharmacol. Ther. 42 (5) (2015) 515–528.

[43] M.T. Sorbara, E.R. Littmann, E. Fontana, T.U. Moody, C.E. Kohout, M. Gjonbalaj, V. Eaton, R. Seok, I.M. Leiner, E.G. J.C.h. Pamer, microbe, Functional and genomic variation between human-derived isolates of Lachnospiraceae reveals inter-and intra-species diversity, Cell Host Microbe. 28 (1) (2020) 134–146. e4.

[44] P.M. Smith, M.R. Howitt, N. Panikov, M. Michaud, C.A. Gallini, Y.M. Bohlooly, J. N. Glickman, W.S. Garrett, The microbial metabolites, short-chain fatty acids, regulate colonic Treg cell homeostasis, Science. 341 (6145) (2013) 569–573.

[45] N. Arpaia, C. Campbell, X. Fan, S. Dikiy, J. van der Veeken, P. deRoos, H. Liu, J. R. Cross, K. Pfeffer, P.J. Coffer, A.Y. Rudensky, Metabolites produced by commensal bacteria promote peripheral regulatory T-cell generation, Nature. 504 (7480) (2013) 451–455.

[46] X. Zhang, D. Yu, D. Wu, X. Gao, F. Shao, M. Zhao, J. Wang, J. Ma, W. Wang, X. Qin, Y. Chen, P. Xia, S. Wang, Tissue-resident Lachnospiraceae family bacteria protect against colorectal carcinogenesis by promoting tumor immune surveillance, Cell Host Microbe. 31 (3) (2023) 418–432 e8.

[47] H. Guo, W.C. Chou, Y. Lai, K. Liang, J.W. Tam, W.J. Brickey, L. Chen, N. D. Montgomery, X. Li, L.M. Bohannon, A.D. Sung, N.J. Chao, J.U. Peled, A.L. C. Gomes, M.R.M. van den Brink, M.J. French, A.N. Macintyre, G.D. Sempowski, X. Tan, R.B. Sartor, K. Lu, J.P.Y. Ting, Multi-omics analyses of radiation survivors identify radioprotective microbes and metabolites, Science. 370 (6516) (2020).

[48] N. Reichardt, S.H. Duncan, P. Young, A. Belenguer, C. McWilliam Leitch, K.P. Scott, H.J. Flint, P. Louis, Phylogenetic distribution of three pathways for propionate production within the human gut microbiota, ISME J. 8 (6) (2014) 1323–1335.

[49] H. Sonowal, A. Saxena, S. Qiu, S. Srivastava, K.V. Ramana, Aldose reductase regulates doxorubicin-induced immune and inflammatory responses by activating mitochondrial biogenesis, Eur. J. Pharmacol. 895 (2021) 173884.

[50] J.K. Jadapalli, G.W. Wright, V. Kain, M.A. Sherwani, R. Sonkar, N. Yusuf, G. V. Halade, Doxorubicin triggers splenic contraction and irreversible dysregulation of COX and LOX that alters the inflammation-resolution program in the myocardium, Am. J. Physiol. Heart Circ. Physiol. 315 (5) (2018) H1091–H1100.

[51] S.S. Bansal, M.A. Ismahil, M. Goel, B. Patel, T. Hamid, G. Rokosh, S.D. Prabhu, Activated T lymphocytes are essential drivers of pathological remodeling in ischemic heart failure, Circ Heart Fail. 10 (3) (2017) e003688.
[52] F.J. Carrillo-Salinas, N. Ngwenyama, M. Anastasiou, K. Kaur, P. Alcaide, Heart inflammation: immune cell roles and roads to the heart, Am. J. Pathol. 189 (8) (2019) 1482–1494.
[53] M.V. Singh, M.W. Chapleau, S.C. Harwani, F.M. Abboud, The immune system and hypertension, Immunol. Res. 59 (1–3) (2014) 243–253.
[54] J.L. Estall, D.J. Drucker, Glucagon-like Peptide-2, 26, 2006, pp. 391–411.